Organic Electronics 34 (2016) 139–145

Contents lists available at ScienceDirect

Organic Electronics

journal homepage: www.elsevier.com/locate/orgel

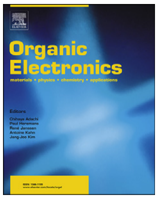

High performance black-to-transmissive electrochromic device with panchromatic absorption based on TiO_2-supported viologen and triphenylamine derivatives

Duo Weng, Yuchen Shi, Jianming Zheng*, Chunye Xu*

Hefei National Laboratory for Physical Sciences at Microscale, CAS Key Laboratory of Soft Matter Chemistry, Department of Polymer Science and Engineering, University of Science and Technology of China, Hefei 230026, PR China

ARTICLE INFO

Article history:
Received 21 February 2016
Received in revised form
16 April 2016
Accepted 16 April 2016
Available online 22 April 2016

Keywords:
Black-to-transmissive
Electrochromic device
Viologen
Triphenylamine
Stability
Chemisorption

ABSTRACT

A novel black-to-transmissive electrochromic device based on TiO_2-supported viologen and triphenylamine derivatives was designed and constructed via the absorption-complementary approach. In the device, cathodically coloring electrochromic material 1,4-bis[((*N*-phosphono-2-ethyl)-4,4′-bipyridinium)-methyl]-benzene tetrachloride acted as working electrode and novel anodically coloring electrochromic material (4-((4-(dimethylamino)-phenyl)(4-methoxyphenyl)-amino)-benzyl) phosphonic acid acted as counter electrode. The assembled electrochromic device achieved panchromatic absorption over entire visible spectrum with almost zero transmittance in colored state. The optical contrast (ΔT) of the device realized in this work was comparable to the highest value (60%) among all reported black-to-transmissive ECDs. Furthermore, excellent cycling stability was achieved, which maintained almost 80% of the initial ΔT value at 570 nm after continuous 100,000 switchings. These outstanding comprehensive electrochromic performances potentially make this device a promising candidate for electrochromic device applications.

1. Introduction

Electrochromism, which refers to a reversible optical absorbance/transmittance change in response to an externally applied potential, has been developing over several decades. In the electrochromic system, electrochemical redox reactions result in a reversible variation of transmitted/reflected light and color change of electroactive materials [1–3]. Past few years have witnessed great advances and gradual applications of electrochromic materials especially for electrochromic devices (ECDs), such as automatic anti-glazing mirror [4], sunglasses [5] and switchable displays [6,7], as well as e-paper [8] and "smart windows" [8–10].

Electrochromic devices (ECDs) with efficient controllability and excellent stability are particularly desirable for practical applications. Color change is of great significance among the properties of ECDs which can be used in many fields. Although much study about different colored-to-transmissive electrochromic devices such as three primary colors (RGB) [11–13], purple [14] and magenta [15] have been investigated so far, achievement of black-to-transmissive switchable electrochromic devices still remains a challenging task. The reason for that is partly due to the complexity for rendering materials absorbing efficiently over visible spectrum (400–750 nm) in colored state, and fully bleaching out in the same region in bleached state. To date, two primary strategies can be used to achieve this goal. One is to synthesize an individual polymer or copolymer, which serves as a single working electrode absorbing across the whole visible region. Typical example by this method would be a chemical copolymer with substituted donor-acceptor system developed by Reynolds group [16,17]. All reported polymers exhibit good black-to-transmissive switching with high optical contrast, yet the stability of the fabricated ECD is insufficient. The other strategy is based on "color-mixing" theory bearing the blends or multilayers to achieve complementary absorption. A reported device combines four absorption-complementary electrochromic polymers (red, green, blue, and yellow), and is capable of generating dark color [18]. However, relatively low optical contrast of 25% poses a big obstacle to its practical application. These two strategies mentioned above are both based on electrochromic polymers, while the stability of ECD

---

* Corresponding authors.
E-mail addresses: jmz@ustc.edu.cn (J. Zheng), chunye@ustc.edu.cn (C. Xu).

http://dx.doi.org/10.1016/j.orgel.2016.04.028

is insufficient or optical contrast is not satisfactory.

In this work, we designed a black-to-transmissive ECD based on viologen and triphenylamine derivatives with excellent optical performance and outstanding stability. Our group has been devoted ourselves in EC field for a long time [19,20]. It is found that viologen and triphenylamine are two commonly used small organic molecules with distinct electrochromic performances. Viologen is one type of electrochromic cathodic materials with reversible optical color change between dication state (V^{2+}, bleached) and radical cation state ($V^{+\bullet}$, colored). The color of viologen can be controlled through modifying substituent group [21–25]. Comparing with viologen, triphenylamine as anodic electrochromic material, can be easily oxidized to form stable polarons attributed to electron-rich characteristics, while resulting in a noticeable change in color [26–28]. Based on the "color mixing" theory, it claims that if two color stimuli are mixed, the resulting color will lie somewhere along a straight line connecting two points on the chromaticity diagram [29]. Herein, we utilized the coloring mixing strategy and selected blue and yellow-green as complementary colors. Specifically, we synthesized two color-complementary viologen and triphenylamine derivatives, 1,4-bis[((*N*-phosphono-2-ethyl)-4,4′-bipyridinium)-methyl]-benzene tetrachloride (PBT) and a new material (4-((4-(dimethylamino)-phenyl) (4-methoxyphenyl)-amino)-benzyl) phosphonic acid (DBP). They exhibited blue and yellow-green respectively and the absorption of PBT and DBP might complement in visible region. Then the black-to-transmissive switching electrochromic device was produced by the combination of PBT and DBP materials.

The absorption, optical, redox behaviors and electrochemical properties of PBT and CBP electrodes were characterized and discussed below. An electrochromic device (ECD) with these two materials was fabricated, and its electrochromic performance and cycle stability were investigated as well.

2. Experiment

2.1. Materials and instrumentation

All chemicals used in this work were commercial products and used as received without further purification. The material for the electrolyte, propylene carbonate (PC), ethylene carbonate (EC) and lithium hexafluorophosphate ($LiPF_6$) were purchased from Sigma Aldrich Chemical. Toluene was dried by refluxing with CaH_2.

NMR spectra were measured by Bruker Avance AV400. Infrared (IR) spectra were recorded on a Nicolet 8700 Fourier-transform infrared (FT-IR) spectrometer. Ultraviolet-visible NIR (UV-vis-NIR) spectra were obtained by JASCO V-670 spectrophotometer. Cyclic voltammograms were collected using CHI 660D electrochemical analyzer with a three-electrode cell using a film (2 cm × 2 cm) on fluorine-doped indium oxide glasses (FTO) as working electrode, a silver wire as reference electrode and a platinum wire as counter electrode. Spectroelectrochemical analysis was performed by the combination of CHI 660D electrochemical analyzer and UV-vis-NIR spectrophotometer. Photographs of the films and devices were taken with a Canon (IXUS 125 HS) digital camera.

2.2. Materials synthesis

2.2.1. Preparation of 1,4-bis[((N-phosphono-2-ethyl)-4,4′-bipyridinium)-methyl]-benzene tetrachloride (PBT)

The synthesis route of compound PBT was performed following sequential process reported by Taya, M. group [25]. First, 1-diethyl ethylphosphonate-4,4′-bipyridinium bromide (1) was prepared by mixing 4,4′-bipyridine (2 g, 12.8 mmol) and diethyl bromoethyl phosphonate (3.14 g, 12.8 mmol) in acetone (20 ml) in a 100 ml round-bottomed flask and heated under stirring at 50 °C until the solid precipitate was formed. The precipitate was filtered. The filtrate was heated again and the process was repeated until no more solid formed. The as-obtained precipitate was washed with ether and dried under vacuum to pale yellow product (3 g, 58%). Then, 1,4-bis[((*N*-diethylphosphono-2-ethyl)-4,4′-bipyridinium)-methyl]-benzene tetrabromide (2) was prepared by mixing the above product (2 g, 4.99 mmol) and 1,4-bis(bromomethyl) benzene (0.657 g, 2.49 mmol) in acetonitrile (50 ml) in a 100 ml round bottomed flask and refluxed under stirring for 24 h. The resulting precipitate was filtered and washed with ether and hot acetonitrile, then dried under vacuum to yield 2.2 g of yellow product. Finally, 1,4-bis[((*N*-Phosphono-2-ethyl)-4,4′-bipyridinium)-methyl]-benzene tetrachloride (3) was obtained by adding the above product (2 g, 1.88 mmol) to hydrochloric acid solution (40 ml) and allowed to reflux for 24 h under stirring. The solvent was removed under vacuum and the compound was crystallized with ethanol, filtered and dried in the vacuum to yield 1.7 g of pale yellow product. The main synthesis process was shown in Scheme 1.

1: ^1H NMR (300 MHz, D_2O, ppm): δ 1.09–1.13 (t, 6H), 2.62–2.73 (t, 2H), 3.95–4.05 (q, 4H), 4.81–4.91 (t, 2H), 7.82–7.84 (d, 2H), 8.35–8.37 (d, 2H), 8.66–8.68 (d, 2H), 8.92–8.94 (d, 2H).

2: ^1H NMR (300 MHz, D_2O, ppm): δ 1.16–1.21 (t, 12H), 2.70–2.81 (t, 4H), 4.02–4.11 (q, 8H), 5.25–5.38 (t, 4H), 6.25 (s, 4H), 7.48 (s, 4H), 7.72–7.81 (d, 2H), 8.25–8.32 (d, 2H), 8.76–8.83 (d, 2H), 9.62–9.70 (d, 2H).

3: ^1H NMR (300 MHz, D_2O, ppm): δ 2.30–2.41 (t, 4H), 4.77–4.86 (t, 4H), 5.87 (s, 4H), 7.51 (s, 4H), 8.41–8.45 (m, 8H), 9.04–9.06 (m, 8H).

2.2.2. Preparation of (4-((4-(dimethylamino)-phenyl) (4-methoxyphenyl)-amino)-benzyl) phosphonic acid (DBP)

The synthesis route of a new compound DBP is described as follows. In the first step, 4-bromo-N, *N*-dimethylphenylamine (3.0 g, 15 mmol), *p*-anisidine (2.02 g, 16.5 mmol), sodium *tert*-butoxide (2.016 g, 20.97 mmol), tris(dibenzylideneacetone)dipalladium (0.27 g, 0.299 mmol) and tri-*tert*-butyphosphine (0.12 g, 0.59 mmol) were added to a three-neck flask, followed by 60 ml dry toluene. The mixture was heated at 90 °C with stirring for 24 h in argon atmosphere. Then the solvent was removed and the crude product was dissolved by chloroform. The mixture was washed with sodium chloride solution and the organic phase was dried by $MgSO_4$. Finally, 1.5 g of orange oily liquid (4) was obtained by column chromatograghy. (Yield: 47%)

In the second step, compound 4 (1.5 g, 6.19 mmol), 4-bromobenzaldehyde (1.65 g, 8.97 mmol), tris(dibenzylideneacetone)dipalladium (0.11 g, 0.12 mmol), tri-*tert*-butylphosphine (0.054 g, 0.25 mmol) and cesium carbonate (2.7 g, 8.30 mmol) were mixed to dry toluene (50 mL) and heated under agitation at 90 °C for 24 h in argon atmosphere. Then the solvent was removed and the product was dissolved by chloroform. After filtering the mixture, the filtrate was washed with saturated sodium chloride solution and the organic phase was dried by $MgSO_4$. Finally, 1.8 g of orange-yellow oily liquid (5) was obtained by column chromatograghy. (Yield: 72%)

In the third step, compound 5 (1.8 g, 5.20 mmol) and sodium borohydride (0.26 g, 7.26 mmol) were dissolved in 50 mL THF in argon atmosphere and refluxed at 70 °C for 24 h. Then the mixture was extracted by diethyl ether and the collected organic phase was dried by $MgSO_4$. Next, the compound 6 was obtained by evaporating the solvent. (Yield: 86%)

In the fourth step, 1.6 g of compound 6, 5 mL triethyl phosphate, and 0.8 g $ZnBr_2$ were added into a flask and stirred at room temperature under argon atmosphere. After 24 h, HCl/CH_3OH was added into the mixture and stirred for 10 h. The solution was

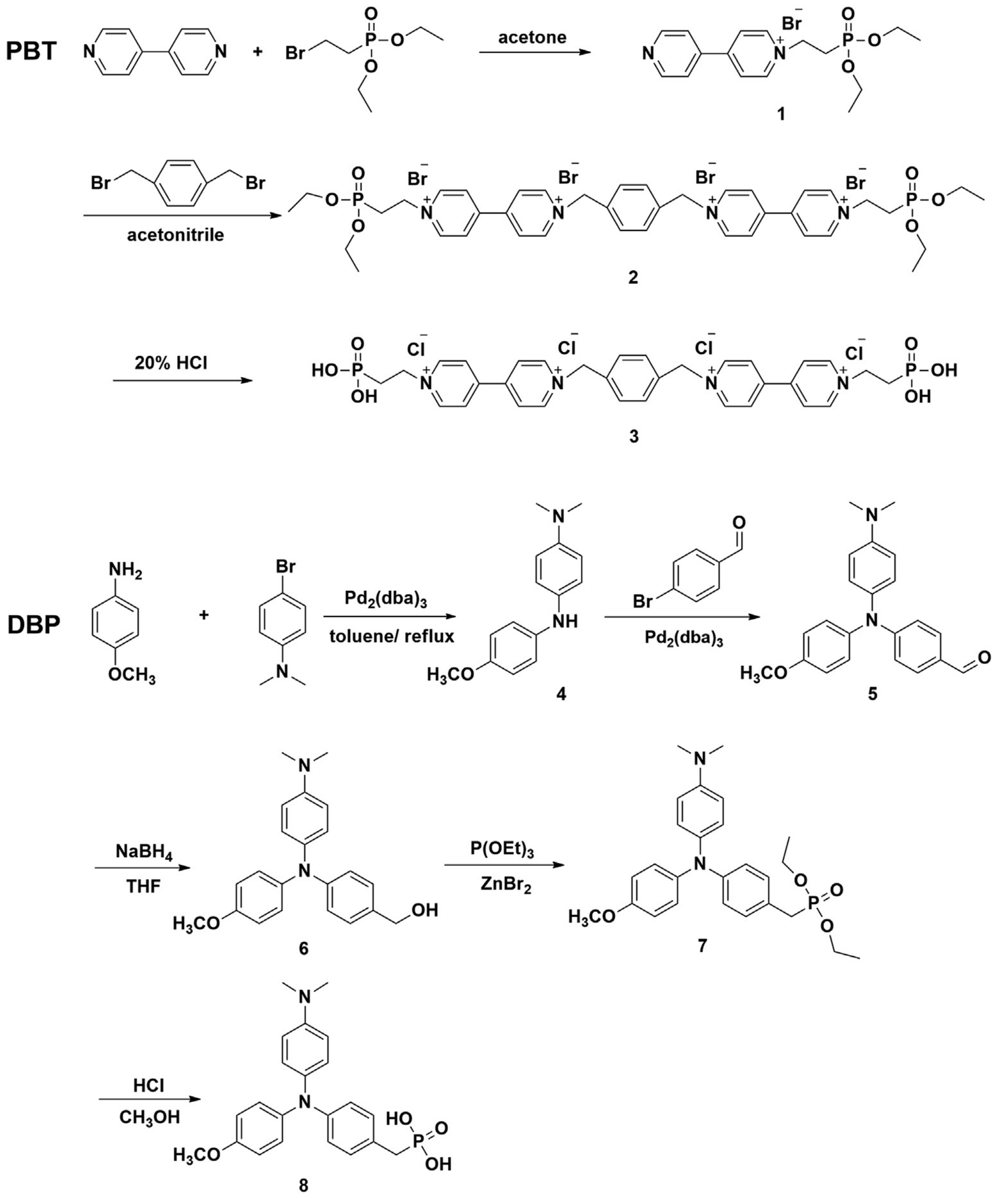

Scheme 1. Synthesis route of PBT and DBP.

filtered and washed by H_2O and CH_2Cl_2. We obtained 0.5 g almost colorless viscous liquid (8). (Yield: 37%) The main synthesis process was shown in Scheme 1. The ^1H NMR and FT-IR characterizations of PBT and DBP were detailed in supporting information (see Fig. S1-S10).

4: ^1H NMR (300 MHz, $CDCl_3$, ppm): δ 2.81–2.83 (s, 6H), 3.50–3.55 (d, 3H), 4.30–4.35 (s, 1H), 6.59–6.92 (m, 8H).

5: ^1H NMR (300 MHz, $CDCl_3$, ppm): δ 2.94 (s, 6H), 3.74 (s, 3H), 6.62–6.65 (d, 2H), 6.74–6.77 (d, 2H), 6.80–6.83 (d, 2H), 6.90–7.02 (d, 2H), 7.05–7.09 (d, 2H), 7.52–7.55 (d, 2H), 9.663 (s, 1H).

6: ^1H NMR (300 MHz, $CDCl_3$, ppm): δ 2.85 (s, 6H), 3.71 (s, 3H), 4.50 (s, 2H), 6.60–6.63 (d, 2H), 6.70–6.75 (d, 2H), 6.82–6.85 (d, 2H), 6.93–7.02 (m, 4H), 7.06–7.09 (d, 2H).

7: ^1H NMR (300 MHz, $CDCl_3$, ppm): δ 1.09–1.15 (t, 6H), 2.83 (s, 2H), 3.36–3.43 (m, 6H), 3.68 (s, 3H), 3.61–3.65 (m, 4H), 6.57–6.63 (d, 2H), 6.80–6.85 (d, 2H), 6.90–6.97 (m, 4H), 7.04–7.07 (d, 2H).

8: ^1H NMR (300 MHz, $CDCl_3$, ppm): δ 2.78–2.89 (s, 6H), 3.71–3.75 (s, 3H), 3.94–4.07 (d, 2H), 6.71–6.83 (m, 4H), 6.91–7.00 (m, 6H), 7.15–7.19 (m, 2H).

2.3. Fabrication of ECD

2.3.1. Electrodes

TiO_2 paste was spread onto fluorine-doped tin oxide glass (FTO, 14Ω/□, Nippon Sheet Glass, Japan) with doctor-blade method and then baked at 450 °C for 30 min to obtain nanoparticle TiO_2 films, with thickness of 1 μm and transmittance above 80% on light wavelength of 400–800 nm TiO_2 Films were immersed in either PBT/H_2O (0.03 M) or DBP/CH_2Cl_2 (0.03 M) solution for 24 h for chemisorption. After removing the solution, the prepared PBT/TiO_2 and DBP/TiO_2 electrodes were all stored in a glovebox before use. The SEM characterizations of electrodes were provided in Fig. S11.

2.3.2. Electrolyte

PC/EC/$LiPF_6$ solution was chosen as electrolyte. The concentration of $LiPF_6$ was 0.1 M, and the volume ratio of PC: EC was 1:1. The electrolyte was bubbled with argon for 4 h and stored in a glovebox.

2.3.3. *Assembly*

Fig. 1 illustrates an exploded schematic of the ECD design, which is assembled as follows. The cell was fabricated in a glove box under argon atmosphere in order to avoid any moisture and oxygen contamination. A parafilm (100 μm thickness) was cast onto the DBP electrode and pressed together with the PET electrode. The parafilm was employed as a spacer for sealing the device tightly and keeping 100 μm thickness of the electrolyte. After gelation, the edges of the device were sealed by UV-curable sealant.

3. Results and discussion

3.1. *Visible absorption spectra of electrodes*

Absorbance spectral analysis was performed to investigate detailed absorption properties of PBT and DBP electrodes in visible region. As illustrated in Fig. 2, the absorption of cathodically coloring blue PBT material effectively covered the range of 500–650 nm and the absorption peak was distributed on 556 nm. As for anodically coloring yellow green DBP material on the opposite electrode, it revealed two absorption peaks at 456 nm and 715 nm respectively, which maximally compensated absorption regions less than 500 nm and greater than 650 nm. Thereby, the total absorption spectra of PBT and DBP electrodes nearly covered the entire range of visible spectrum, which indicated that the combination of PBT and DBP inside an ECD could achieve the goal with broad and effective absorption in visible region.

3.2. *Electrochemical properties of electrodes*

The electrochemical properties of PET and DBP electrodes were investigated with cyclic voltammetry (CV). As displayed in Fig. 3(a) and (b), the PBT electrode was reduced to blue state when the voltage reached −1.0 V, and was oxidized to transparent state as the potential increased to −0.3 V. Conversely, the DBP counter electrode was oxidized to yellow green state when the voltage reached 1.0 V, and was reduced back to transparent at the voltage of 0.3 V. Besides, charge-matching is essential between working electrode and counter electrode for a complementary ECD. The two electrodes PBT and DBP demonstrated the matching charge capacity, which can be justified by integrating the current density in the CV curves. Thus, the CV curves exhibited that the similar redox potential value with opposite polarity and matching charge capacity of two electrodes, representing they could complement each other and match well to fabricate an ECD.

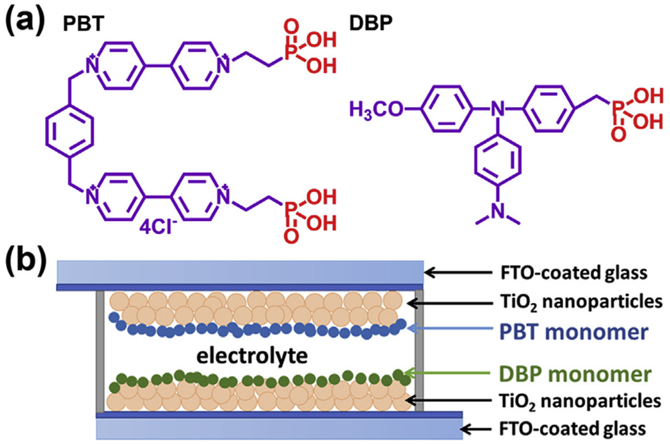

Fig. 1. (a) Chemical structure of PBT and DBP, and (b) schematic of device based on PBT and DBP electrodes.

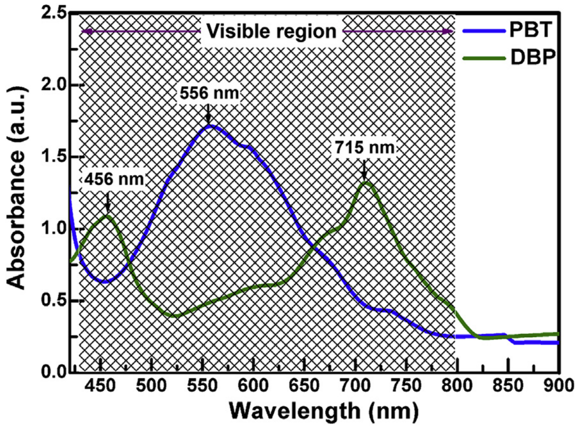

Fig. 2. Visible absorption spectra of PBT and DBP electrodes of their colored states in PC/EC/$LiPF_6$ (0.1 M).

Furthermore, detail optical properties of PBT and DBP electrodes were characterized by spectroelectrochemical experiments when ±0.3 V and ±1.0 V had been applied. Fig. 3(c) and (d) present the transmittance curves of PBT and DBP electrodes in different state, respectively. As shown, in their transparent states, PBT electrode (−0.3 V) exhibited high transmittance of 85% from 500 to 750 nm and DBP electrode (0.3 V) displayed satisfactory transmittance of 65% from 560 to 750 nm as well. In their dark states, the PBT (−1.0 V) and DBP (1.0 V) electrodes both demonstrated effective absorption in visible region with relatively low transmittance (deep color), with the minimums of T% below 10%. Here, we defined transmittance change (ΔT %) of EC device:

$$\Delta\%T = T^t(\lambda) - T^d(\lambda)$$

T^t (λ) and T^d (λ) represent the light transmittance of certain wavelength λ in the transparent and dark states, respectively. As calculated in Fig. 3(c) and (d), the ΔT% of PBT electrode located at 570 nm reached up to 75% and the DBP electrode attained 60% at the wavelength of 570 nm. These high values further indicated that the fabricated ECD with PBT and DBP electrodes could achieve high optical contrast and effective absorption in visible region with deep transmittance in colored state.

3.3. *Performance of ECD*

3.3.1. *Electrochemical properties of ECD*

To investigate the electrochemical properties and appropriate operation parameters of ECD, an electrochemical analysis with cyclic voltammetry (CV) was performed. As shown in Fig. 4. The device changed to its colored state during the cathodic scan. When the voltage reached −1.5 V, the device was fully colored and exhibited deep black color. As the opposite potential increasing, the device began to bleach and oxidized to its transparent state at the voltage of 0.5 V. Consequently, the fabricated ECD could be darkened by applying a potential of −1.5 V on the working electrode of PBT and be bleached at a potential of 0.5 V, which is an appropriate potential applied to the assembled ECD.

3.3.2. *Electrochromic properties of ECD*

The prepared PBT and DBP electrode materials were employed to fabricate an ECD. Fig. 5(a) and (b) represent the photos of ECD in its transparent and dark states. Applied with - 1.5 V, the ECD transformed to dark state resulting a deep black color, with PBT and

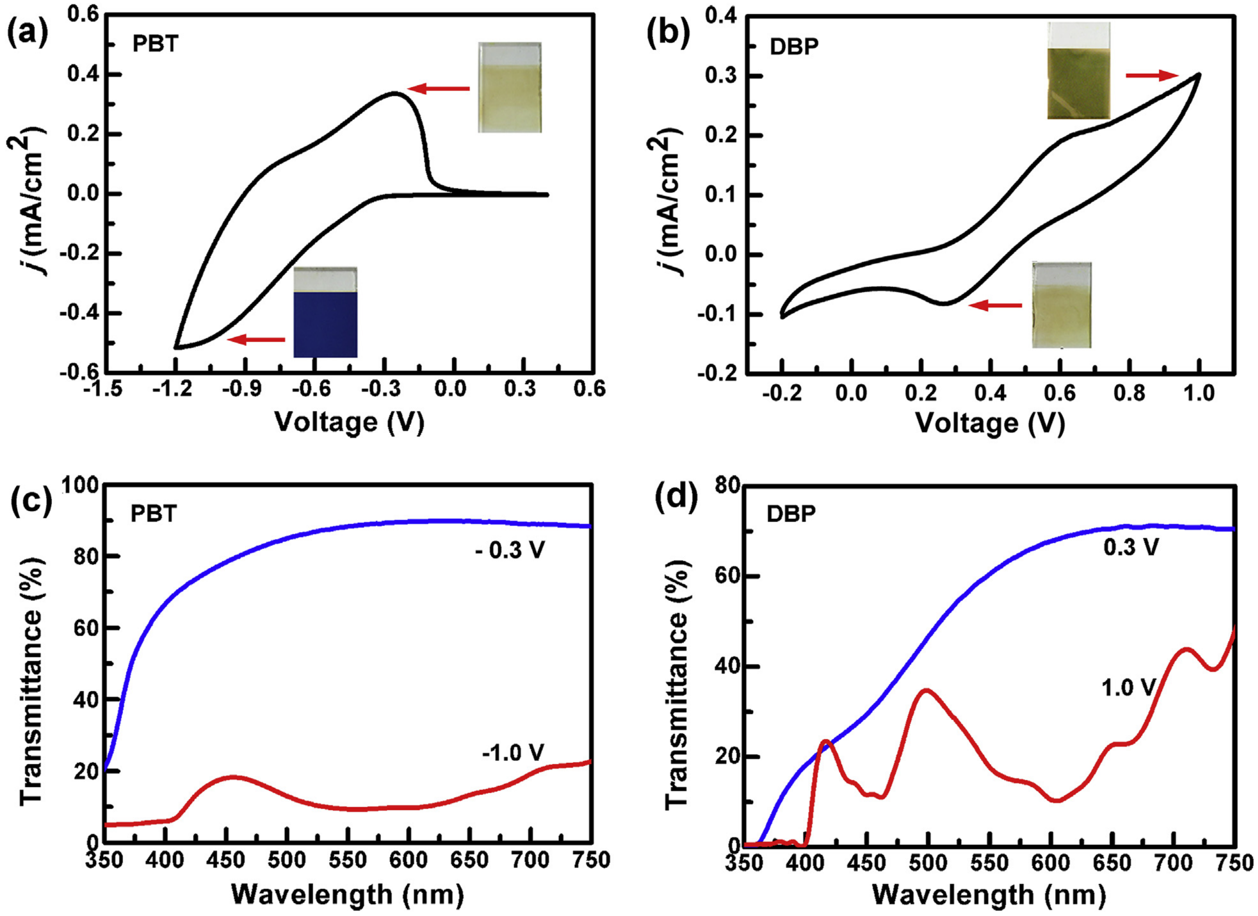

Fig. 3. Cyclic voltammograms of (a) PBT and (b) DBP electrode with PC/EC/LiPF$_6$ (0.1 M) as supporting electrolyte. (Scan rate = 50 mV s^{-1}). Transmittance spectra of (c) PBT electrode and (d) DBP electrode in transparent and dark states at different voltage.

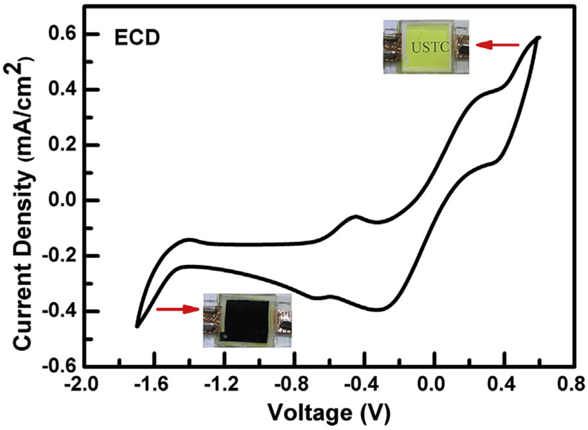

Fig. 4. Cyclic voltammograms of ECD with PC/EC/LiPF$_6$ (0.1 M) as electrolyte. (Scan rate = 50 mV s^{-1}). Insert: the photos of ECD in transparent and dark state.

CBP materials in their reduced state (deep blue) and oxidized state (yellow green) respectively. With the opposite potential of 0.5 V applying, the ECD became transparent immediately, accompanied with the PBT and DBP materials returned to their oxidized states and reduced state. Apparently, the character "USTC" under the ECD became invisible completely when the ECD switched to its dark state as exhibited in Fig. 5(b).

The transmittance spectra of the fabricated ECD was also measured as illustrated in Fig. 5(c). High transmittance of over 50% from 500 to 800 nm could be observed in transparent state. Conversely, the device demonstrated complete spectra absorption approaching almost zero transmittance in dark state. The

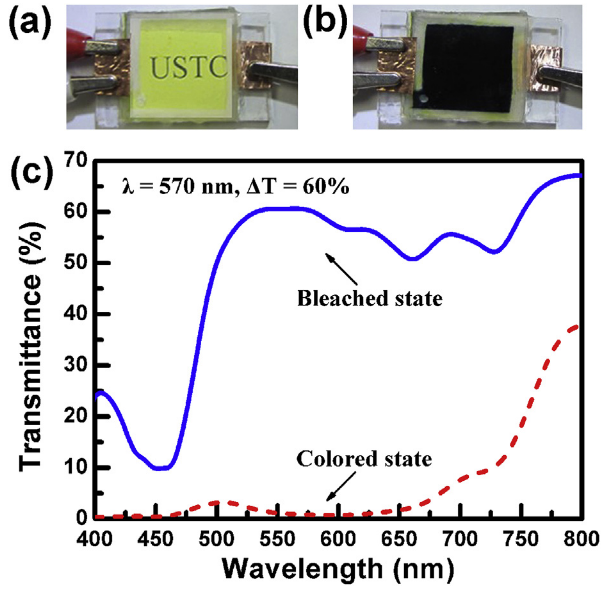

Fig. 5. Photos of ECD (2 cm × 2 cm) in (a) transparent state, (b) dark state, and (c) transmittance spectra of ECD in extreme states of highly absorptive and highly transmissive.

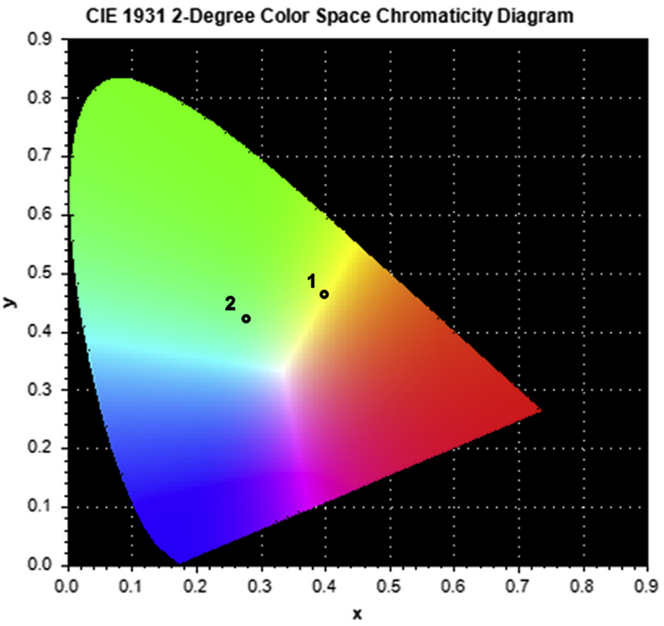

Fig. 6. Colorimetry (x–y diagram) of ECD (1) in the bleached state (0 V) and (2) in the colored states (- 1.5 V).

Table 1
Numerical chromaticity coordinates CIE (*x, y and* $\%Y_L$) for ECD in transparent and dark state.

ECD state	*x*	*y*	$\%Y_L$
Transparent state	0.384	0.461	56%
Dark state	0.278	0.425	1.4%

transmittance curves confirmed that the ECD achieved a satisfactory optical contrast of 60% located at 570 nm and made a black-to-transmissive device a reality.

To scientifically evaluate the color change of ECD occurring on electrochemical switching, the ECD was subjected to colorimetric analysis by using CIE 1931 system of colorimetry. The color of ECD is represented quantitatively using three attributes “x” (the red-blue ratio), “y” (the green-blue ratio) and $\%Y_L$ (the relative or percentage luminance). Fig. 6 depicts the CIE color space plots for the device described in this research and the CIE 1931 numerical data (x, y, $\%Y_L$) was given in Table 1. When the device was in transparent state, the chromaticity coordinates ($x = 0.384$, $y = 0.461$, $\%Y_L = 56\%$) were closed to D55 illuminant ($x = 0.332$, $y = 0.348$, $\%Y_L = 100\%$) [30], which demonstrated that the ECD was capable to reach a highly transmissive state. Moreover, the point of transparent state located at light yellow region according to the chromaticity coordinates, which corresponded to the photo of ECD. In dark state, the value of x, y, and $\%Y_L$ ($x = 0.278$, $y = 0.425$, $\%Y_L = 1.4\%$) all decreased, which indicated the color of ECD had changed. Besides, the point of colored state located in the mixed region of blue and yellow green, because the ECD was composed by blue colored PET electrode and yellow green colored DBP electrode. Furthermore, the value of $\%Y_L$ decreased as low as 1.4%, which suggested the ECD could achieved a deep black color. This provides further evidence that the color change of the ECD is nearly from transparent to black.

3.3.3. *Electrochromic switching properties*

Electrochromic switching parameters of the ECD were investigated by the combination of a double step chronoamperometry technique and an UV-vis-NIR spectrophotometer. The results were revealed in Fig. 7. We defined response time as the time needed by ECD to achieve 90% of its transmittance changes. The two-step potentials, the response time and the ΔT were exhibited in Fig. 7. As illustrated, the device could switch rapidly between its transparent and dark states. As calculated in Fig. 7(b), the switching time of the device (2 cm × 2 cm) was less than 4 s (3.0 s) during the coloring process and 5 s (4.8 s) during the bleaching process. The switching time was affected by the diffusion rate of Li^+ dissolved in electrolyte and the amount of electron, which was driven by the applied voltage. The higher applied voltage, the shorter switching time. In our experiment, the bleached voltage required for the ECD was relatively lower than the colored voltage from the CV curve, so we chose 0.5 V for bleaching and −1.5 V for coloring. Thus, the time for bleaching process was relatively longer than the coloring process. Overall, the quick speed of the response time was due to the well matching of two electrodes. In addition, chemisorptions between phosphonic acid and TiO_2 nanoparticles made electrochromic materials tightly adhesive to conductive substrates, consequently leading electrons to transfer into the FTO glass-TiO_2 nanoparticles-electrochromic materials quickly.

3.3.4. *Stability properties*

The long-term stability upon cycling played a key role on the electrochromic performance of the devices. Therefore, the electrochemical stability of device was investigated by switching between the two-step of −1.5 V (5 s) and 0.5 V (10 s) for 120 K cycles. We recorded the light transmittances at 570 nm after 10 K, 30 K, 60 K, 90 K and 120 K cycles, respectively. As shown in Fig. 8, no

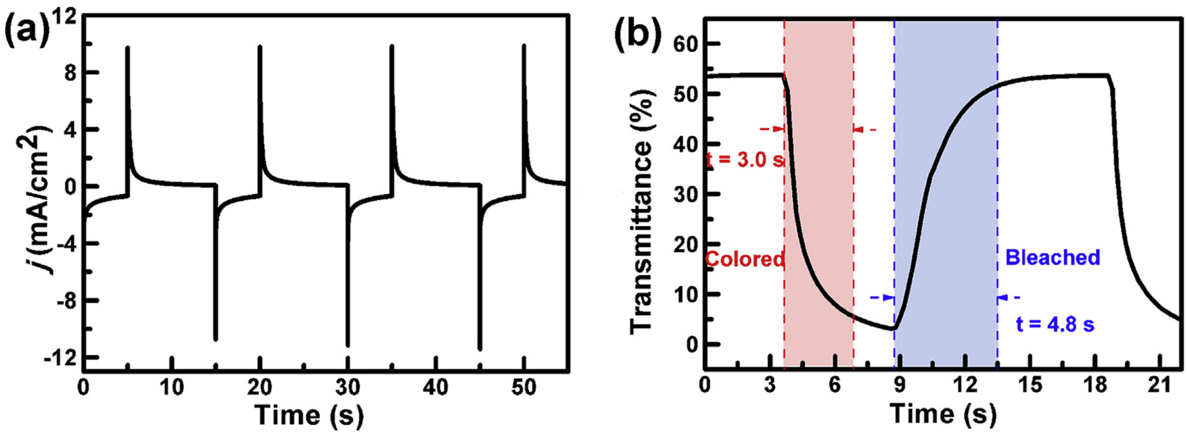

Fig. 7. Electrochromic switching and transmittance changes of ECD (−1.5 V to color, 0.5 V to bleach) at its $\Delta \lambda_{max}$ on FTO glass-TiO_2 nanoparticles substrates in PC/EC/$LiPF_6$ (0.1 M).

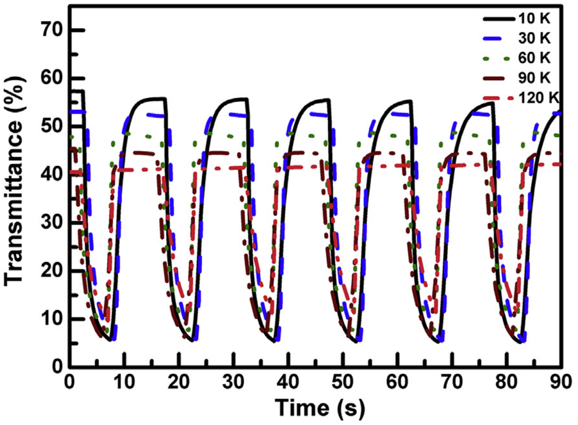

Fig. 8. Long-term switching of ECD at 570 nm after various cycles (10 K, 30 K, 60 K, 90 K and 120 K cycles, K: 1000 times).

appreciable change in the response time was observed, while the shape of the curves changed a little. The light transmittance response at 570 nm was 57.0%–5.0% after 10 K cycles and 45.2%–5.8% after 120 K cycles respectively. The device still remained a relatively stable state, with an optical contrast loss of 20% after 120 K cycles. Thus, the fabricated ECD exhibited stable high contrast and response even after continuous 120,000 switchings, indicating it was potential for practical electrochromic applications such as smart windows and anti-glare mirrors.

4. Conclusions

In this paper, a novel black-to-transmissive switching electrochromic device based on viologen and triphenylamine derivatives via the absorption-complementary approach was successfully designed, fabricated and characterized by our group. The ECD was assembled with viologen-modified TiO_2 electrode and a new triphenylamine-modified TiO_2 electrode. The new designed anodically material DBP realized the matching spectra absorption and redox potential with cathodically material PBT. The combination of PBT and DBP materials inside an ECD achieved panchromatic absorption over entire visible spectrum. In addition, it also exhibited satisfactory ΔT% through the visible region with ΔT_{max} of 60% at 570 nm ($T_b = 60.1\%$ and $T_d = 0.1\%$) and excellent stability up to 120,000 cycles. These outstanding properties endow the assembled ECD with great potential to incorporate into both window-type and display-type electrochromic devices.

Acknowledgements

We gratefully acknowledge financial supports of this work by the National Natural Science Foundation of China (21274138, 21474096 and 21273207). The authors are also grateful to Dr. Chihlong Chiang and Dr. Fengyu Su, former postdoctoral fellows for their pioneering work on this research.

Appendix A. Supplementary data

Supplementary data related to this article can be found at http://dx.doi.org/10.1016/j.orgel.2016.04.028.

References

[1] P.R. Somani, S. Radhakrishnan, Electrochromic materials and devices: present and future, Mater. Chem. Phys. 77 (2003) 117–133.
[2] D.R. Rosseinsky, R.J. Mortimer, Electrochromic systems and the prospects for devices, Adv. Mater. 13 (2001) 783–793.
[3] P. Monk, R. Mortimer, D. Rosseinsky, Electrochromism and Electrochromic Devices, Cambridge University Press 2007.
[4] E. Redel, J. Mlynarski, J. Moir, A. Jelle, C. Huai, S. Petrov, M.G. Helander, F.C. Peiris, G. von Freymann, G.A. Ozin, Electrochromic Bragg mirror: ECBM, Adv. Mater 24 (2012) OP265–269.
[5] A.M. Osterholm, D.E. Shen, J.A. Kerszulis, R.H. Bulloch, M. Kuepfert, A.L. Dyer, J.R. Reynolds, Four shades of brown: tuning of electrochromic polymer blends toward high-contrast eyewear, ACS Appl. Mater. Interfaces 7 (2015) 1413–1421.
[6] V.K. Thakur, G. Ding, J. Ma, P.S. Lee, X. Lu, Hybrid materials and polymer electrolytes for electrochromic device applications, Adv. Mater 24 (2012) 4071–4096.
[7] P. Andersson Ersman, J. Kawahara, M. Berggren, Printed passive matrix addressed electrochromic displays, Org. Electron. 14 (2013) 3371–3378.
[8] D. Corr, Coloured electrochromic “paper-quality” displays based on modified mesoporous electrodes, Solid State Ionics 165 (2003) 315–321.
[9] S.-M. Wang, L. Liu, W.-L. Chen, E.-B. Wang, High performance visible and near-infrared region electrochromic smart windows based on the different structures of polyoxometalates, Electrochimica Acta 113 (2013) 240–247.
[10] C. Xu, L. Liu, S.E. Legenski, D. Ning, M. Taya, Switchable window based on electrochromic polymers, J. Mater. Res. 19 (2011) 2072–2080.
[11] A. Durmus, G.E. Gunbas, P. Camurlu, L. Toppare, A neutral state green polymer with a superior transmissive light blue oxidized state, Chem. Commun. (2007) 3246–3248.
[12] A.L. Dyer, M.R. Craig, J.E. Babiarz, K. Kiyak, J.R. Reynolds, Orange and red to transmissive electrochromic polymers based on electron-rich dioxythiophenes, Macromolecules 43 (2010) 4460–4467.
[13] M. Li, Y. Sheynin, A. Patra, M. Bendikov, Tuning the electrochromic properties of poly (alkyl-3, 4-ethylenedioxyselenophenes) having high contrast ratio and coloration efficiency, Chem. Mater. 21 (2009) 2482–2488.
[14] B.D. Reeves, C.R. Grenier, A.A. Argun, A. Cirpan, T.D. McCarley, J.R. Reynolds, Spray coatable electrochromic dioxythiophene polymers with high coloration efficiencies, Macromolecules 37 (2004) 7559–7569.
[15] A. Tsuboi, K. Nakamura, N. Kobayashi, Multicolor electrochromism showing three primary color states (cyan–magenta–yellow) based on size- and shape-controlled silver nanoparticles, Chem. Mater. 26 (2014) 6477–6485.
[16] P. Shi, C.M. Amb, E.P. Knott, E.J. Thompson, D.Y. Liu, J. Mei, A.L. Dyer, J.R. Reynolds, Broadly absorbing black to transmissive switching electrochromic polymers, Adv. Mater 22 (2010) 4949–4953.
[17] P.M. Beaujuge, S. Ellinger, J.R. Reynolds, The donor-acceptor approach allows a black-to-transmissive switching polymeric electrochrome, Nat. Mater. 7 (2008) 795–799.
[18] H. Shin, Y. Kim, T. Bhuvana, J. Lee, X. Yang, C. Park, E. Kim, Color combination of conductive polymers for black electrochromism, ACS Appl. Mater. interfaces 4 (2012) 185–191.
[19] S. Mi, J. Wu, J. Liu, Z. Xu, X. Wu, G. Luo, J. Zheng, C. Xu, AIEE-Active and electrochromic bifunctional polymer and a device composed thereof synchronously achieve electrochemical fluorescence switching and electrochromic switching, ACS Appl. Mater. Interfaces 7 (2015) 27511–27517.
[20] Z. Xu, X. Chen, S. Mi, J. Zheng, C. Xu, Solution-processable electrochromic red-to-transmissive polymers with tunable neutral state colors, high contrast and enhanced stability, Org. Electron. 26 (2015) 129–136.
[21] R. Cinnsealach, G. Boschloo, S.N. Rao, D. Fitzmaurice, Electrochromic windows based on viologen-modified nanostructured TiO 2 films, Sol. Energy Mater. Sol. Cells 55 (1998) 215–223.
[22] B. Gadgil, P. Damlin, T. Ääritalo, C. Kvarnström, Electrosynthesis of viologen cross-linked polythiophene in ionic liquid and its electrochromic properties, Electrochimica Acta 133 (2014) 268–274.
[23] J. Palenzuela, A. Viñuales, I. Odriozola, G. Cabañero, H.J. Grande, V. Ruiz, Flexible viologen electrochromic devices with low operational voltages using reduced graphene oxide electrodes, ACS Appl. Mater. Interfaces 6 (2014) 14562–14567.
[24] C. Pozo-Gonzalo, M. Salsamendi, A. Viñuales, J.A. Pomposo, H.-J. Grande, Highly transparent electrochromic plastic device that changes to purple and to blue by increasing the potential, Sol. Energy Mater. Sol. Cells 93 (2009) 2093–2097.
[25] Y. Rong, S. Kim, F. Su, D. Myers, M. Taya, New effective process to fabricate fast switching and high contrast electrochromic device based on viologen and Prussian blue/antimony tin oxide nano-composites with dark colored state, Electrochimica Acta 56 (2011) 6230–6236.
[26] K. Choi, S.J. Yoo, Y.-E. Sung, R. Zentel, High contrast ratio and rapid switching organic polymeric electrochromic thin films based on triarylamine derivatives from layer-by-layer assembly, Chem. Mater. 18 (2006) 5823–5825.
[27] L.-C. Lin, H.-J. Yen, Y.-R. Kung, C.-M. Leu, T.-M. Lee, G.-S. Liou, Novel near-infrared and multi-colored electrochromic polybenzoxazines with electroactive triarylamine moieties, J. Mater. Chem. C 2 (2014) 7796.
[28] S. Beaupré, J. Dumas, M. Leclerc, Toward the development of new textile/plastic electrochromic cells using triphenylamine-based copolymers, Chem. Mater. 18 (2006) 4011–4018.
[29] G. Sonmez, C.K.F. Shen, Y. Rubin, F. Wudl, A red, green, and blue (RGB) polymeric electrochromic device (PECD): The Dawning of the PECD Era, Angew. Chem. 116 (2004) 1524–1528.
[30] R.J. Mortimer, T.S. Varley, In situ spectroelectrochemistry and colour measurement of a complementary electrochromic device based on surface-confined Prussian blue and aqueous solution-phase methyl viologen, Sol. Energy Mater. Sol. Cells 99 (2012) 213–220.